Two long-wave infrared spectral polarimeters for use in understanding polarization phenomenology

Stephanie H. Sposato
Matthew P. Fetrow
Air Force Research Laboratory
Space Vehicles Directorate
3550 Aberdeen SE
Kirtland Air Force Base, New Mexico 87117

Kenneth P. Bishop, MEMBER SPIE
Applied Technology Associates
1900 Randolph SE
Albuquerque, New Mexico 87106

Thomas R. Caudill, MEMBER SPIE
Air Force Research Laboratory
Space Vehicles Directorate
3550 Aberdeen SE
Kirtland Air Force Base, New Mexico 87117

Abstract. Spectrally varying long-wave infrared (LWIR) polarization measurements can be used to identify materials and to discriminate samples from a cluttered background. Two LWIR instruments have been built and fielded by the Air Force Research Laboratory: a multispectral LWIR imaging polarimeter (LIP) and a full-Stokes Fourier transform infrared (FTIR) spectral polarimeter (FSP), constructed for higher spectral resolution measurements of materials. These two instruments have been built to gain an understanding of the polarization signatures expected from different types of materials in a controlled laboratory and in varying field environments. We discuss the instruments, calibration methods, general operation, and measurements characterizing the emitted polarization properties of materials as a function of wavelength. The results show that we are able to make polarization measurements with a relative accuracy of 0.5% degree of polarization (DOP) between two different instruments that are calibrated with the same techniques, and that these measurements can improve the understanding of polarization phenomenology.
[DOI: 10.1117/1.1464870]

Subject terms: polarimeters; long-wave infrared; polarized light; polarization.

Paper 010163 received May 10, 2001; revised manuscript received Dec. 7, 2001; accepted for publication Dec. 10, 2001.

1 Introduction

The phenomenon of polarized light has been understood for some time, but its usefulness in material identification is just being revealed. Reflection and emission of electromagnetic radiation from a variety of materials produces partially polarized light when viewed at off-normal angles. Electromagnetic radiation will become polarized after reflection off a smooth surface, as described by the Fresnel equations. According to Kirchoff's law relating absorption and emission, thermal emission will also show some polarization with a preference to electric field components oriented parallel to the surface normal.

In 1824, Arago[1] made the first empirical observation of partially polarized light thermally emitted from an incandescent body. Subsequently, Millikan[2] performed experiments with various metals and dielectrics. He observed that the highest partial polarization of emission occurred for angles most oblique to the surface normal. Also, he noted that metals have considerably higher partial polarization than dielectrics, and that for a given material type, partial polarization was highest for a smooth surface condition.

One advantage of polarization is that it can provide improved contrast for a number of sample detection and discrimination applications. Emissive polarization can possibly be used to find a hidden object in an isothermal scene where conventional infrared (IR) sensors would detect little or no contrast. Polarization also has the potential to distinguish between natural and man-made materials. Man-made, or refined, materials tend to produce a significant polarization content in both reflected and emitted light due to reflection from smooth, often painted, surfaces.[3] Surfaces viewed at normal incidence usually produce unpolarized light. Light reflected from a surface tends to favor s-polarization, polarization perpendicular to the plane of incidence, while light emitted from the same surface tends toward p-polarization, polarization parallel to the plane of incidence. Also, surface roughness generally tends to reduce the amount of polarization. In the natural environment, thermal IR radiance is generally unpolarized, with water being one of the only natural materials to exhibit polarization. Long-wave infrared (LWIR) data of water show s-polarization in regions of sun glint, but elsewhere p-polarization is observed. For a cold, clear sky, the LWIR signal is p-polarized up to 10% at large incidence angles.[4]

To further investigate polarization phenomenology, Air Force Research Laboratory (AFRL) constructed two long-wave IR spectral polarimeters, and performed experiments in the laboratory and in the field at Kirtland Air Force Base, New Mexico. The two instruments are designed with a rotating quarter-waveplate and a fixed linear analyzer as the polarization optics to make a complete Stokes measurement. This type of polarimeter was chosen because it has a straightforward calibration, is flexible in design, and inexpensive. The results of this work show that we are able to make polarization measurements with a relative accuracy to 0.5% degree of polarization (DOP) between two different instruments calibrated with similar techniques, and they

Report Documentation Page

Form Approved
OMB No. 0704-0188

1. REPORT DATE	2. REPORT TYPE	3. DATES COVERED
MAY 2002	**N/A**	**-**

4. TITLE AND SUBTITLE	5a. CONTRACT NUMBER
Two Long-Wave Infrared Spectral Polarimeters for Use in Understanding Polarization Phenomenology	5b. GRANT NUMBER
	5c. PROGRAM ELEMENT NUMBER
6. AUTHOR(S)	5d. PROJECT NUMBER
	5e. TASK NUMBER
	5f. WORK UNIT NUMBER
7. PERFORMING ORGANIZATION NAME(S) AND ADDRESS(ES) **Air Force Research 3550 Aberdeen Avenue SE Kirtland AFB, NM 87117-5776**	8. PERFORMING ORGANIZATION REPORT NUMBER
9. SPONSORING/MONITORING AGENCY NAME(S) AND ADDRESS(ES)	10. SPONSOR/MONITOR'S ACRONYM(S)
	11. SPONSOR/MONITOR'S REPORT NUMBER(S)

12. DISTRIBUTION/AVAILABILITY STATEMENT
Approved for public release, distribution unlimited

13. SUPPLEMENTARY NOTES

14. ABSTRACT

15. SUBJECT TERMS

16. SECURITY CLASSIFICATION OF:			17. LIMITATION OF ABSTRACT	18. NUMBER OF PAGES	19a. NAME OF RESPONSIBLE PERSON
a. REPORT	b. ABSTRACT	c. THIS PAGE			
unclassified	**unclassified**	**unclassified**	**UU**	**10**	

Standard Form 298 (Rev. 8-98)
Prescribed by ANSI Std Z39-18

demonstrate the usefulness of polarimetry for material identification.

2 LWIR Instruments

The Air Force Research Laboratory has conducted experiments to measure the spectral and polarization characteristics of various materials using two distinct LWIR devices: a LWIR imaging polarimeter (LIP) and a FTIR spectral polarimeter (FSP). The two instruments are of a standard design, utilizing a rotating quarter-waveplate and a fixed linear analyzer to make a complete Stokes measurement. The four Stokes components are calculated using the data reduction method (DRM) described by Chipman.[5] The two drawbacks of an instrument of this design are the requirement of a static scene during the measurement time and the spectral dependence of the waveplate retardance. Because of this, the experiments are carefully conducted to limit scene variability. Estimates of scene and instrument drift are included as sources of error in the data. Also, careful calibrations are performed to determine the retardance of the waveplate as a function of wavelength. Background subtraction and polarization calibration are important as well.

2.1 *LWIR Imaging Polarimeter*

The LWIR imaging polarimeter (LIP) performs a complete Stokes measurement by using the combination of a rotating quarter-waveplate and a stationary linear analyzer. Due to cost and time constraints when building the polarimeter, uncooled polarization optics and lenses were used. The system was designed around an off-the-shelf mini Dewar IR camera with a 256×256 pixel HgCdTe focal plane array (FPA) having a long-wave cutoff at 9.6 μm. The FPA has a few thousand bad pixels, and approximately 10% pixel-to-pixel nonuniformity before correction.

A nonuniformity correction (NUC) is performed with off-the-shelf software to compensate for different responses of pixels using a two-point linear correction. A cold uniform object and then a warm uniform object are placed in front of the camera lens at different times to determine each pixel's response. A linear curve is fit to each pixel separately. This function is then used to convert the raw analog-to-digital (A/D) counts read from the FPA to the corrected counts, which are recorded by the controlling computer.

The camera has a wideband cold filter between 8.2 and 12.0 μm, and four selectable warm spectral bands between 8.2 and 9.5 μm. A 100-mm focal length four-element lens assembly with an f number of 2.3 is mounted on the front of the camera. A schematic of the LIP is shown in Fig. 1. Light passes through the lens to the quarter-waveplate where it is retarded, and then through the stationary wire grid polarizer. Next, the light passes through the selected warm spectral filter. After this, the light enters the cooled-optics portion of the instrument. The Dewar has a coated ZnSe window with a cold shield of f number 2.3. The light then passes through the cold filter to the FPA. The system sits on a $2\times1'$ optical breadboard that can be mounted on a tripod.

Any one of the five uncooled narrow-band spectral filters mounted on a bar can be consecutively placed directly behind the polarizer to obtain multispectral data. Figure 2 shows the bandpass of the warm spectral filters used in this

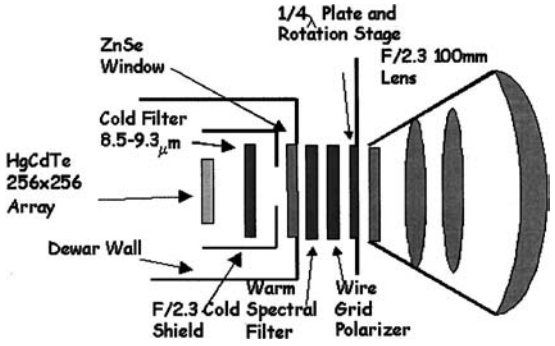

Fig. 1 Schematic of the LIP.

experiment with the modeled response of the FPA. The FPA relative response curve was modeled using the manufacturer's data and calibration measurements were made with an extended set of bandpass filters. The filter curves were measured with a FTIR spectrometer.

The quarter-waveplate is a one-inch diameter, achromatic net zero-order, CdS/CdSe retarder. The system makes polarization measurements by collecting a series of camera frames while the quarter-waveplate is rotated through a fixed number of positions. The rotation of the waveplate is motorized and computer controlled. The number of fixed locations is variable. A standard collection sequence consists of a series of ten measurements spaced 40-deg apart, with a redundant measurement at 360 deg used to check for drift in the scene. (Collett provides a more detailed explanation of spinning waveplates.[6]) The retardance of the waveplate is shown in Fig. 3 and is discussed further in Sec. 3.4.

Offset measurements are made to remove the background signal emitted from the optical components that would erroneously reduce the measured polarization. The amount of background light is estimated by placing a liquid-N_2-cooled plate in front of the system after each measurement. This plate serves as a uniform cold source that provides a background level or pedestal, representing the bias on the camera and any thermal signal from the

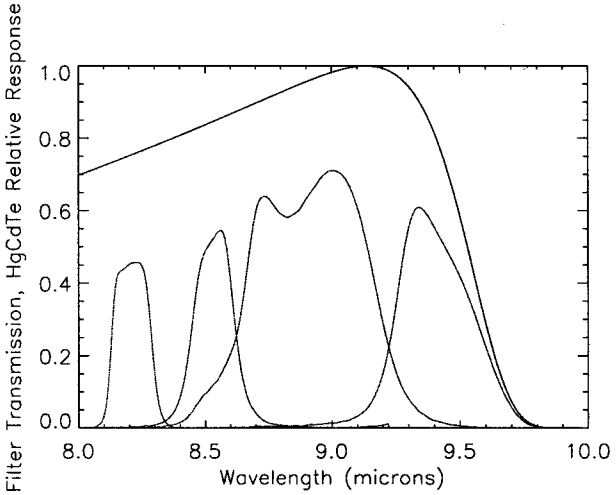

Fig. 2 Modeled spectral response of array and measured bandpass.

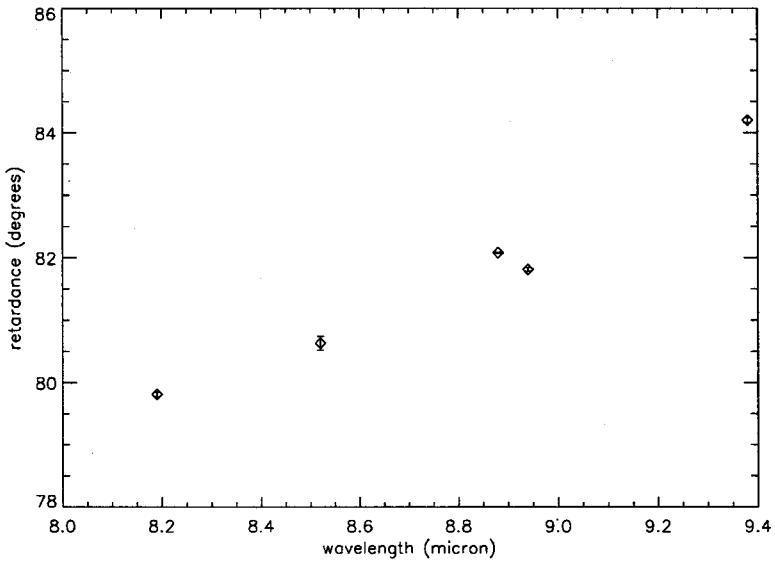

Fig. 3 Retardance as a function of wavelength for the LIP.

optical system. This background frame is subtracted from each frame of real data before analysis. The background measured on the camera has a direct effect on the S_0 element of the Stokes vector, which in turn affects the other Stoke's elements, since all are typically normalized using S_0. Figure 4 shows the temperature profile of the plate after being removed from the liquid N_2 bath. The plate does warm up to approximately 110 K during the 15-sec measurement, but this temperature is still well below the temperature of the LIP optics and is sufficient for background subtraction.

The software running the system is a combination of commercial and custom-made programs. Off-the-shelf software controls the camera, the data acquisition, and the image display. Analog signals from the FPA are amplified in the camera system and digitized with external electronics. Digital signals pass to an I/O board contained in a Pentium II PC. The data are collected in 12-bit camera frames at a rate of 60 Hz. The computer control of the waveplate rotation stage was custom built, with commands being called from inside the camera's macro language. The required amount of time to take a measurement varies according to the number of frames collected at each position of the waveplate. Typically, 32 images are taken at each position and averaged to increase signal to noise. Ignoring the manual placement of the hot, cool, and liquid N_2 measurements, with these settings a single wavelength polarimeter measurement takes approximately 15 sec: 5 sec to collect the data and another 10 sec to spin the waveplate. Specifications for the LIP settings used to collect the data presented are found in Table 1.

The Stokes measurement of a particular scene for a specific filter is computed from the following data. (For the warm/cold/background plates, no intensity change with waveplate position was measured.)

1. Warm plate measurement (64-frame average), 1 waveplate position.
2. Cold plate measurement (64-frame average), 1 waveplate position.
3. Background plate measurement (64-frame average), 1 waveplate position.
4. Nine measurements of the scene, moving the waveplate between 0 and 320 deg in 40-deg steps (each a 32-frame average).

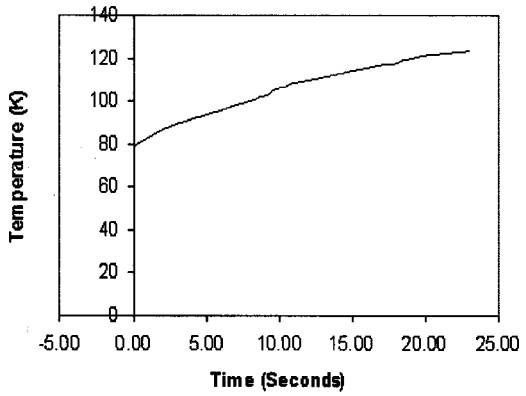

Fig. 4 Plot of temperature changes with time for the liquid N_2 background plate. The measurement begins when the plate is removed from the liquid N_2, and it continues for approximately 15 sec.

Table 1 Specifications for the LIP.

Focal plane array	256×256 pixel HgCdTe
IFOV	0.5 mrad
Waveplate	achromatic CdS/CdSe net zero-order quarter-waveplate
Polarizer	0.5-μm pitch gold grid on AR-coated ZnSe
Frame rate and digitization	60 Hz, 12-bit digitization
Measurement speed	15 sec per Stokes image/bandpass filter

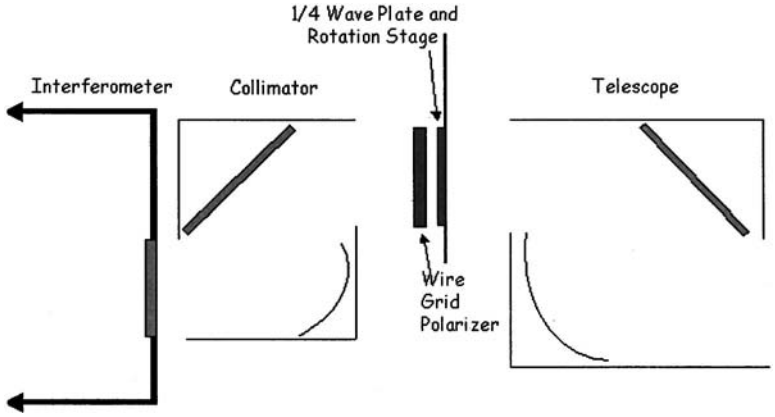

Fig. 5 Schematic of the FSP.

5. Tenth measurement of the scene with the waveplate at 360 deg (32-frame average).

Measurements of the scene at the first and last waveplate positions provide an estimate of scene change or drift during the measurement time. Since a scene change causes significant false polarization signatures, data showing this characteristic are not used in the analysis. A quick-look analysis is performed after each measurement to determine if the data were free of drift for a given scene. The data are processed using custom-made IDL programs. Because the scenes taken with the LIP are complicated and contain many kinds of materials, a region of interest (ROI) analysis is used to evaluate the polarization of individual samples. Uniform ROIs are selected by hand from the sample images. The four Stokes elements are first calculated per pixel and then averaged over the ROI using the DRM. Pixels that did not have a suitable linear response are flagged as bad pixels and are not included in the resultant Stokes values reported for a subregion. Bad pixels are marked by comparison with data from the warm and cool plates. Those not responding to within 10% of all the pixels in the array are removed. The number of bad pixels fluctuates due to the quality of the NUC. Ancillary data, including thermocouple data for tracking sample temperature and weather station data for tracking weather conditions, are stored on a separate computer from the data collection computer.

2.2 *FTIR Spectral Polarimeter*

The FTIR spectral polarimeter (FSP) also collects full-Stokes spectra using a rotating quarter-waveplate and linear polarizer combination. The instrument was developed by adding polarization optics to an off-the-shelf Michelson interferometer. The waveplate is placed at a field-stop location in front of the interferometer. The layout of the instrument is shown in Fig. 5. Light enters the telescope from the right, and is focused by the f/5 reflective telescope onto the net zero-order waveplate. The light passes through the fixed wire grid polarizer, is collimated by another set of reflective f/5 optics, and sent into the interferometer. The telescope has a 2-in aperture, off-axis parabolic, protected aluminum mirror. The waveplate is a half-inch diameter CdS/CdS net zero-order waveplate. The plate is designed for CO_2 laser work, and as such provides nearly 90 deg of retardance at 10.6 μm. The measured retardance of the plate between 8 and 12.5 μm is shown in Fig. 6. Placing the waveplate at the field stop reduces potential image motion when rotating the optic. The waveplate is mounted in a motorized rotation stage, controlled by the data acquisition computer. The wire grid polarizer is fixed to pass horizontally linearly polarized light just behind the rotating waveplate. This component completes the polarization sensitive portions of the instrument. The interferometer, a Bomem MB 200, provides selectable spectral resolution from 2 to 32 wavenumbers, at up to 64 scans per second depending on the resolution selected. Interferograms are detected using a standard single-pixel HgCdTe detector. The detector is sensitive to wavelengths between 8 and 12.5 μm, with the lower limit resulting from atmospheric transmission.

The FSP software consists of a custom control and acquisition program written for a Pentium PC. The software controls the interferometer and the rotation stage, and acquires both interferograms and spectra for each waveplate position. Data are collected by coadding these interferograms and spectra at each of typically 10 waveplate rotation positions around a full circle. Redundant 0- and 360-deg waveplate positions are collected, providing an estimate of scene or sensor drift during the measurement. As with the LIP, warm, cool, and liquid-N_2-cooled plate reference sources are sampled for each Stokes measurement providing calibration and instrument gain and offset information. Also, 32 spectra of data are averaged at each waveplate position. Each spectral Stokes measurement taken with the FSP is computed from the data in the same manner described previously for the LIP instrument, though the FSP has no spatial information. In addition, the FSP data can be spectrally averaged to improve signal to noise. The Stokes values are again computed using DRM. Specifications for the FSP settings used to collect the data presented in this paper are found in Table 2. The measurement speed for the FSP has increased to 35 sec per Stokes spectra, as compared to the LIP's 15 sec per measurement, because the FSP data acquisition program and waveplate motor are slower.

3 Instrument Calibrations

In constructing these two IR instruments, attempts were made to remove sources of error in the polarization mea-

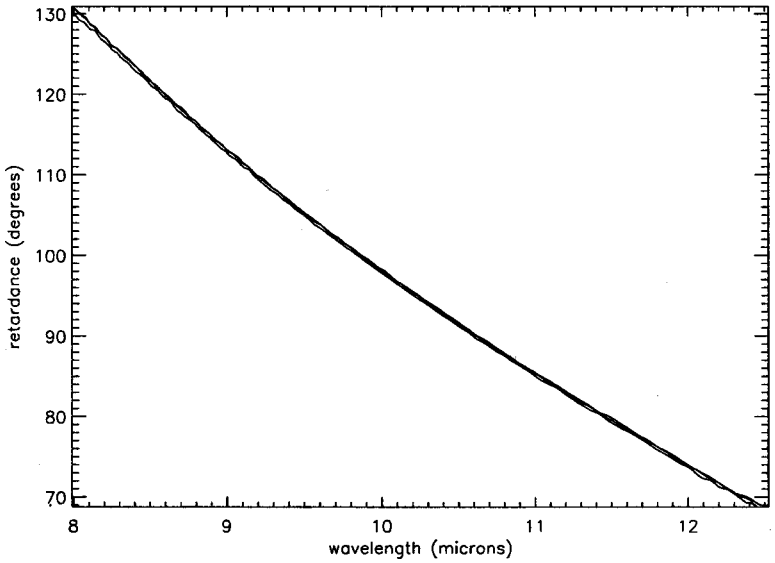

Fig. 6 Retardance as a function of wavelength for the FSP.

surement and to put various diagnostics in place to determine the accuracy and dependability of the instruments. These included determining the polarization contribution of the instrument fore-optics, quantifying the extinction of the wire grid polarizers in the instrument, and performing waveplate calibrations and system checks. An accurate, absolute radiometric calibration was not required for our application. However, relative radiometric calibrations were performed to monitor the status of the instruments. The calibrations and system checks are described in the following two sections.

3.1 *Polarization Contribution of Fore-Optics*

In both the LIP and FSP, light passes through focusing optics before it reaches the polarimeter portion of the instruments. The affect of these optics must be included in the calibration. However, in these polarimeter designs only the optics in front of the instrument, including the wire grid polarizer, can have an effect on the polarization calibration of the instrument. After the polarizer, the sensor only sees horizontal polarization, since the polarizer does not rotate. The polarization affect of the instrument, then, is just represented as another DC term, similar to the thermal signal from the optical system. Both DC terms are measured by placing the liquid-N_2 plate in front of the system, and are then subtracted from the data frames. Also, a modest polarimetric calibration is performed to determine if these optics produce undesirable polarization effects, such as polarization diattenuation, rotation, and retardance.

Table 2 Specifications for the FSP.

Detector	HgCdTe
FOV	28 mrad
Waveplate	net zero-order CdS/CdS
Polarizer	0.5-μm pitch gold grid on AR-coated ZnSe
Spectral range	800 to 1250 cm^{-1} at 4 cm^{-1} resolution
Scan rate and digitization	30 Hz, 16-bit digitization
Measurement speed	35 sec per Stokes spectra

The LIP optics consist of a 100-mm focal length, 4-germanium element antireflective (AR) coated f/2.3 lens assembly. This assembly was not tested separately for polarization effects because it was assumed the refractive components would not induce polarization effects in the LWIR. The FSP fore-optics consist of a two mirror off-axis system made of SiO_2 coated aluminum. This telescope was tested separately for polarization diattenuation, rotation, and retardance effects. Using various laboratory test setups, no polarization effects were found.

3.2 *Extinction of Wire-Grid Polarizers*

The extinction of the wire grid polarizers in the LIP and FSP were checked by comparing the transmission through two polarizers, one inside the instrument and one external, when their axes are aligned versus the transmission when they are crossed. The orientation of the polarizers was measured by illuminating each polarizer with a HeNe laser and measuring the orientation of the diffracted order. The direction of the diffracted orders of light is perpendicular to the grating orientation and parallel to the direction of linear polarization for IR energy passing through. Viewing a 500°C blackbody source through two polarizers, the extinction ratio was measured at greater than 300 to 1 at 8.9 μm.

3.3 *System Checks*

A limited set of known polarization states were input to each instrument as polarization checks. A full Mueller calibration with known polarization states would have been sufficient to determine the full polarization response of the instruments. However, the difficulty in producing quality polarization states in the IR precluded using some states. For each instrument, unpolarized light and linearly polarized light of various orientations were used. The linearly polarized light had a known orientation, but an unknown magnitude, as it was mixed with unpolarized thermal emission from various sources in the laboratory. Using unpolar-

Table 3 Polarimetry biases in the LIP for $S1$.

Filter	Bias (%)
1	−1.0
2	−0.9
3	−0.9
4	−1.2
5	−2.4

ized and linearly polarized light quantifies seven of the sixteen elements of the instruments' polarization response matrix. For the FSP, these checks showed that the instrument is sufficiently close enough to ideal to warrant using the theoretical calibration for the waveplate/polarizer combination. For the LIP, a slight apparent polarization signal was measured when viewing unpolarized sources. This signal, which varied for each filter, surfaced in the S_1 measurement and is listed in Table 3. The signal was treated as a polarization ''bias'' and simply subtracted from all subsequent S_1 measurements of sources that are nearly unpolarized or are polarized to a few percent. In future polarization calibrations, we will try to better assess the source of this polarization effect and properly correct for it in all measured polarizations.

3.4 *Waveplate Calibration*

To measure polarization signatures accurately, it is necessary to quantify how the retardance of the waveplates changes with wavelength. Independent calibrations of the waveplate retardance as a function of wavelength were performed for each LWIR instrument. The method, which was developed at AFRL,[7] involves rotating the waveplates between two linear wire grid polarizers, one in the camera system and one placed in front of a blackbody source. The polarizers are first set so they are aligned with each other and then set crossed with each other. The purpose behind taking two measurements is to remove the DC term resulting from unpolarized light.

The intensity of light after it passes through a waveplate and polarizer is given by

$$S_0' = \frac{1}{2}\left[\left(S_0 + \frac{S_1}{2}\right) + \frac{S_1}{2}\cos(4\omega t) + \frac{S_2}{2}\sin(4\omega t) + S_3\sin(2\omega t)\right], \quad (1)$$

where S_0, S_1, S_2, and S_3 are the four Stokes vector elements of the incident light, and ω is the frequency of the waveplate rotation. The $4\omega t$ term represents the amount of linear polarization created, and the $2\omega t$ term represents the amount of circular polarization created. The DC term results from unpolarized stray light that does not fall in the $4\omega t$ peak or in the $2\omega t$ peak.

This waveplate calibration procedure can be expressed mathematically as follows. When the polarizers are aligned, the matrix equation for the Stokes vector is

$$S_a' = M_H M_{\lambda/4} M_H S. \quad (2)$$

When the polarizers are crossed, the equation is

$$S_c' = M_V M_{\lambda/4} M_H S. \quad (3)$$

In these equations, $M_{\lambda/4}$ is the Mueller matrix for a rotating quarter-waveplate with a retardance of δ, M_H is the Mueller matrix for a horizontal linear polarizer, M_V is the Mueller matrix for a vertical linear polarizer, and S is the Stokes vector representing the polarization state of the light before it passes through the waveplate and polarizers.

The resulting intensity of the light after passing through the waveplate and the aligned polarizers is

$$S_{0a}' = (S_0 + S_1)[1 + \cos^2(2\omega t) + \sin^2(2\omega t)\cos\delta] + \mathrm{DC}, \quad (4)$$

and the intensity of the light after passing through the waveplate and the crossed polarizers is

$$S_{0c}' = (S_0 + S_1)[1 - \cos^2(2\omega t) - \sin^2(2\omega t)\cos\delta] + \mathrm{DC}. \quad (5)$$

Using half-angle formulas, these equations become

$$S_{0a}' = (S_0 + S_1)[\tfrac{3}{2} + \tfrac{1}{2}\cos\delta + \tfrac{1}{2}\cos(4\omega t)(1 - \cos\delta)] + \mathrm{DC} \quad (6)$$

$$S_{0c}' = (S_0 + S_1)[\tfrac{1}{2} - \tfrac{1}{2}\cos\delta - \tfrac{1}{2}\cos(4\omega t)(1 - \cos\delta)] + \mathrm{DC}. \quad (7)$$

The intensity of light from a material measured by a rotating waveplate polarimeter can be written as a truncated Fourier series, similar in form to Eq. (1):

$$I(\omega t) = \tfrac{1}{2}[A + B\sin(2\omega t) + C\cos(4\omega t) + D\sin(4\omega t)]. \quad (8)$$

The coefficients A, B, C, and D, which directly determine the Stokes parameters, can be evaluated using Fourier analysis as follows

$$A = \frac{1}{\pi}\int_0^{2\pi} I(\omega t)\, d(\omega t) \quad (9)$$

$$B = \frac{2}{\pi}\int_0^{2\pi} I(\omega t)\sin(2\omega t)\, d(\omega t) \quad (10)$$

$$C = \frac{2}{\pi}\int_0^{2\pi} I(\omega t)\cos(4\omega t)\, d(\omega t) \quad (11)$$

$$D = \frac{2}{\pi}\int_0^{2\pi} I(\omega t)\sin(4\omega t)\, d(\omega t). \quad (12)$$

For a waveplate calibration, the intensities resulting when the polarizers are aligned and crossed, respectively, are given by Eqs. (6) and (7). By substituting these equations for $I(\omega t)$ in Eqs. (9)–(12), the coefficients (A_a, B_a, C_a, D_a), representing the system with aligned po-

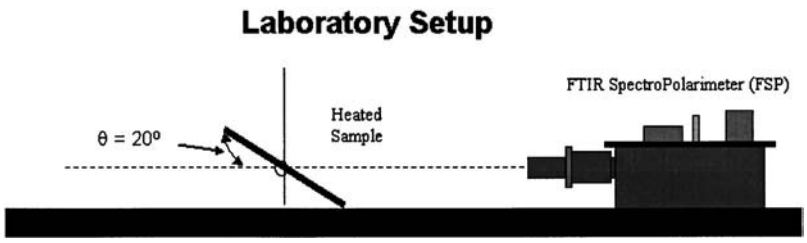

Fig. 7 Laboratory setup for instruments and samples.

larizers, and the coefficients (A_c, B_c, C_c, D_c), representing the system with crossed polarizers, can be determined.

$$A_a = (S_0 + S_1)(\tfrac{3}{2} + \tfrac{1}{2}\cos\delta) + \mathrm{DC} \tag{13}$$

$$C_a = \tfrac{1}{2}(S_0 + S_1)(1 - \cos\delta) \tag{14}$$

$$A_c = (S_0 + S_1)(\tfrac{1}{2} - \tfrac{1}{2}\cos\delta) + \mathrm{DC} \tag{15}$$

$$C_c = -\tfrac{1}{2}(S_0 + S_1)(1 - \cos\delta) \tag{16}$$

$$B_a = B_c = D_a = D_c = 0. \tag{17}$$

These expressions are functions only of constants and the waveplate retardance. The A terms represent the DC value. The C terms represent the amplitude of the $4\omega t$ terms. There are no $2\omega t$ terms, since the polarizers used are linear. For a more detailed explanation of this method of determining the coefficients, see Collett.[6]

The first step in solving for δ is to subtract $A_a - A_c$ to remove the DC term. Then a ratio is taken between the $4\omega t$ terms and the DC terms

$$R = \frac{(C_a - C_c)}{(A_a - A_c)}. \tag{18}$$

Rewriting this using Eqs. (13)–(16) yields

$$R = \frac{(1 - \cos\delta)}{(1 + \cos\delta)} = \frac{\sin^2\left(\frac{\delta}{2}\right)}{\cos^2\left(\frac{\delta}{2}\right)} = \tan^2\left(\frac{\delta}{2}\right), \tag{19}$$

where δ is uniquely determined from this last equation.

The retardance measurements for the LIP were taken on two different days using two different temperature cavity blackbodies as the source. Five measurements at a blackbody temperature of 650 K were taken on the first day, and three were taken at a blackbody temperature of 100 K on the second day. The mean retardance values for each filter are shown in Fig. 3. The error bars, representing random error only, are calculated using the following

$$\frac{t\sigma}{\sqrt{n}}, \tag{20}$$

where σ is the standard deviation, n is the number of retardance measurements, 8, and t is the value corresponding to the 95% confidence limit for a t-distribution, 1.86. A t-distribution rather than a Gaussian distribution best describes the data taken with the LIP, since the number of measurements is less than 30 for each wavelength band.[8]

The three measurements of the retardance for the FSP are shown in Fig. 6. The mean standard deviation of these three measurements was about 0.25 deg.

Experience with this measurement technique has shown mthat up to a 1-deg bias in the retardance measurement can exist, probably due to the optical setup. This is not a very significant problem, however, because a 1-deg change in the retardance will only result in an approximate 0.2% change in polarization for a 5% partially polarized sample. To get a significant change in polarization, the retardance would have to be wrong by at least 4 deg. Separate calibrations were also done looking at the center of the field of view (FOV) versus looking at the edge of the FOV in the LIP. The measured retardances differed by less than 0.5 deg. Lastly, the retardance values as a function of wavelength shown in Fig. 3 agree with retardance measurements made by Sornsin and Chipman[9] and Smith et al.[10] using a similar waveplate.

4 Experiment Results

4.1 *Laboratory Comparison of Instruments*

Various experiments were conducted by the AFRL at Kirtland Air Force Base, New Mexico, to verify the measurement concept and the utility of polarization in material identification/discrimination applications. Polarization experiments are inherently very difficult to make due to the complexity of the instrumentation used; misunderstanding data can lead to erroneous polarization measurements. Because of this, the first experiment was performed in the laboratory to determine if the FSP and LIP, which are of different design, yielded similar polarization estimates looking at the same samples under the same environmental conditions. For this experiment, both instruments were placed on an optics table. The samples were placed at the end of the table, a distance of about five feet from the polarimeters. The three samples, painted aluminum, bare aluminum, and smooth glass, were tilted up to 20 deg from the horizontal, as shown in Fig. 7, and heated to a constant 40°C with strip heaters. The temperature of each sample was maintained with a thermocouple and temperature controller, accurate to 0.1%°C. In actuality, the temperatures varied by a few percent in radiance units. The temperature

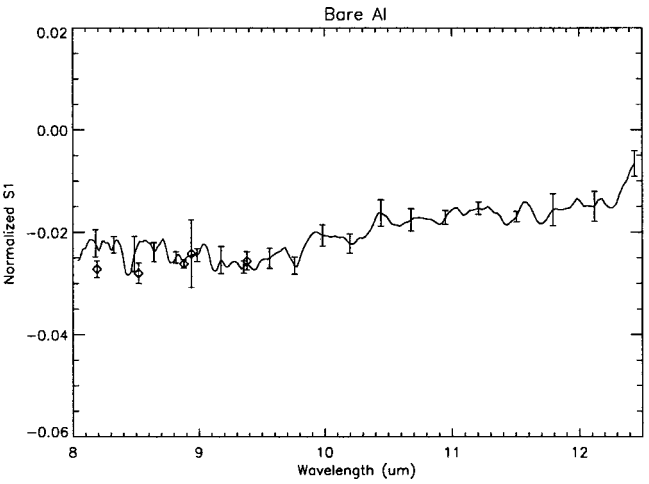

Fig. 8 Normalized $S1$ polarization data for bare aluminum from the FSP (line) and LIP (diamonds) measured in the laboratory.

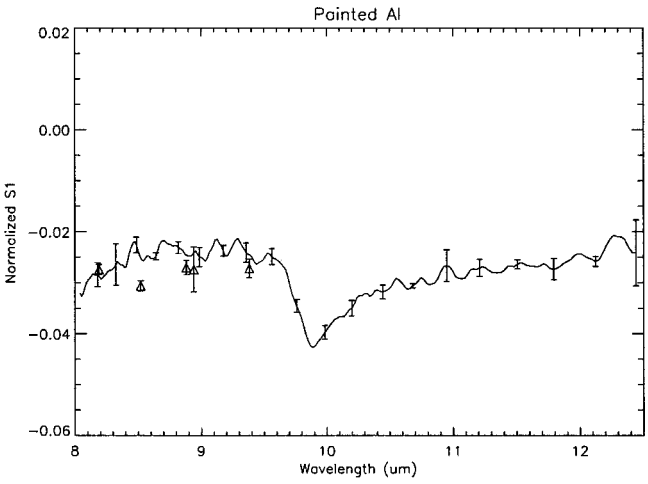

Fig. 9 Normalized $S1$ polarization data for painted aluminum from the FSP (line) and LIP (triangles) measured in the laboratory.

uniformity of the targets was checked using the LIP and found to be sufficient for these measurements. The optics table had a cover over it, but no additional attempt was made to control the environment or reduce room reflections onto the samples. The room temperature was 23°C. Each of the samples was measured with each instrument five times. All the samples fit within the FOV of the LIP, while the samples were placed overfilling the FSP FOV alternately. Also, the small distance to the samples required measuring them with the FSP and LIP at different times.

Figure 8 shows the normalized $S1$ polarization measured from the bare aluminum plate at a 20-deg view angle. The smooth curve is from the FSP, while the five diamonds represent the polarization signal measured with each filter of the LIP. The FSP data has been smoothed to 16 cm^{-1} spectral resolution. The error bars represent the 95% confidence limit in the standard deviation of the mean calculated from the five measurements for each instrument. [See Eq. (20) and the explanation following for more information.] The error bars only include random sources of error and not instrument biases, such as residual errors in the measured waveplate retardance. The modest vertical polarization shown in Fig. 8 is to be expected due to the small thermal contrast between radiation from the laboratory being reflected off the bare aluminum and the radiation emitted from the plate.

Figure 9 shows the measured FSP and LIP polarization for the same aluminum plate painted with a flat, tan paint. The measured normalized $S1$ polarization is similar to that of the bare aluminum measured under the laboratory conditions, though the painted aluminum shows a prominent spectral-polarization feature at about 10 μm. Figure 10 shows the normalized $S1$ data for the smooth glass sample. Note the widely varying polarization signature measured with both instruments, which peaks at around 10 μm. This polarization spectrum results from changes in the complex index of refraction of glass over this wavelength range. Values for normalized $S2$ and $S3$ were negligible for the bare and painted aluminum plates and the glass sample. The laboratory experiment proved to be successful, since both the FSP and LIP yielded similar values of normalized $S1$, $S2$, and $S3$ for all the samples measured. This verified the ability of the FSP and LIP to make comparable polarization measurements of simple samples.

4.2 *Field Survey of Material Polarization*

Measurements of the spectral-polarization characteristics of a variety of common materials were also conducted outdoors from a 20-foot tower, at the south end of Kirtland Air Force Base, New Mexico. The primary goal of these experiments was to quantify the magnitude of polarization and spectral change in polarization of simple materials in an uncontrolled environment. The measurements were made in June during the day under mostly clear skies. The FSP and LIP instruments were placed side by side, and the materials viewed at an angle of 34 deg down from the horizontal, as shown in Fig. 11. Each material was homogeneous and large enough to fill the FOV of the FSP. About 30 different materials were measured; most materials were measured with the FSP 3 to 10 times to gain information about random errors.

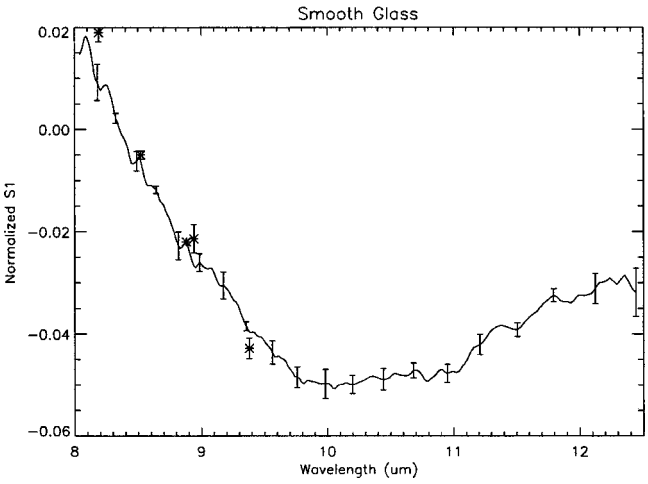

Fig. 10 Normalized $S1$ polarization data for smooth glass from the FSP (line) and LIP (asterisks) measured in the laboratory.

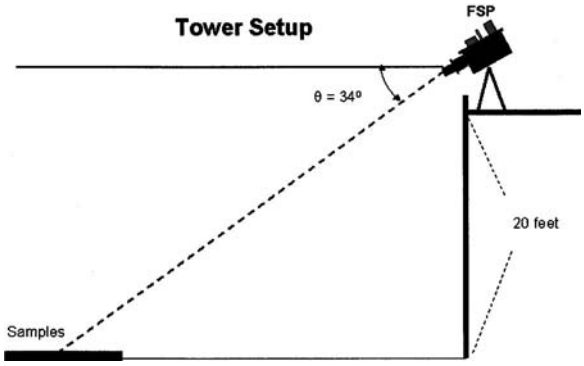

Fig. 11 Setup at outside tower for instruments and samples.

Sample data from the materials survey experiment are shown in Figs. 12, 13, and 14. Plotted in Fig. 12 is normalized $S1$ measured from three samples: an aluminum plate painted with Krylon black paint, a rusted steel plate, and a smooth glass plate. The FSP data have been smoothed to $16\,\mathrm{cm}^{-1}$ resolution. The error bars for the Krylon black plate and rusted steel plate are calculated from five measurements made over a 15-min period, while the error bars for the glass plate are calculated from ten measurements made over a 90-min period. Again, the LIP and FSP show similar polarization values for all the samples. From the figure it is clear that the three materials, Krylon black, rusted steel, and glass, have unique spectral-polarimetric features that could be used for distinguishing one material from the other. Also, one can see the atmosphere reflected in the glass signature, especially the ozone feature. Figures 13 and 14 show the scaled $S2$ and $S3$ data from the same three materials. The data are plotted in exactly the same way as the $S1$ data described before, with the only exception being the expansion of the Y-axis scale for Figs. 13 and 14. Note that there is no significant $S2$ polarization for these materials at the measurement geometry. Also, no significant $S3$ polarization was observed.

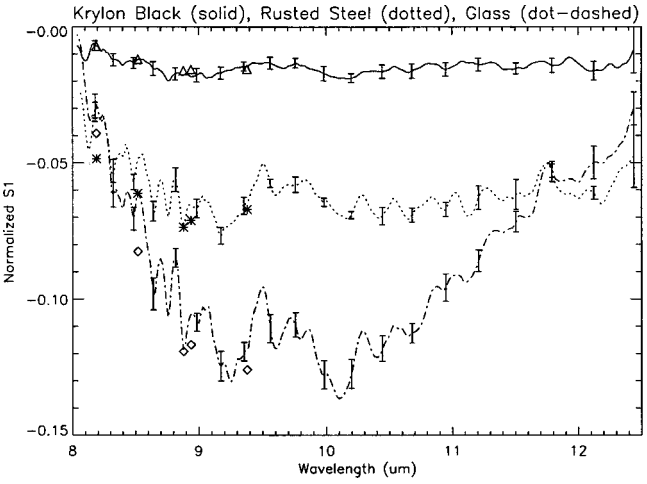

Fig. 12 Normalized $S1$ from three samples measured by the FSP and LIP at the Kirtland tower. Krylon black: solid line=FSP, triangles =LIP. Rusted steel: dotted line=FSP, asterisks=LIP. Glass: dot-dashed line=FSP, diamonds=LIP.

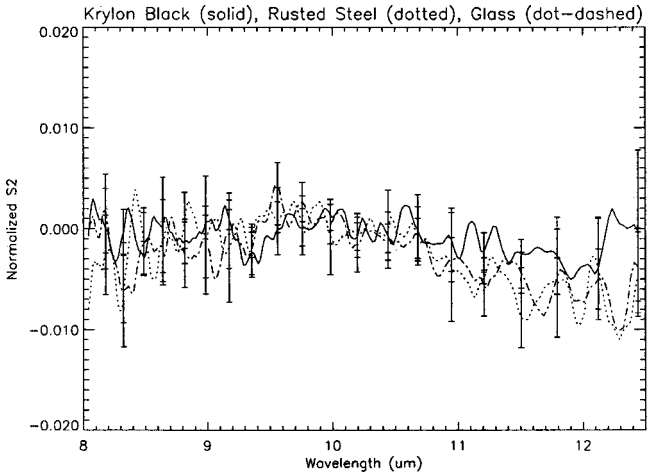

Fig. 13 Normalized $S2$ from three samples measured by the FSP at the Kirtland tower. Krylon black: solid line. Rusted steel: dotted line. Glass: dot-dashed line.

5 Summary

The spectral-polarization characteristics of materials may prove useful in identifying materials and in discriminating samples from a cluttered background. However, an understanding of the polarization expected from various materials in controlled and natural environments must first be ascertained. To this end, two experiments have been performed at AFRL using two LWIR polarimeters with different designs and capabilities: the LIP, a multispectral LWIR imaging polarimeter, and the FSP, a full-Stokes Fourier transform IR spectral polarimeter. The objective of the first experiment, performed in the laboratory, was to compare data from these two instruments. This test was found to be successful in that the data from both instruments agree to within error bars. In the second experiment, performed in the field, the spectral-polarization signatures of common materials were surveyed. The data show that significant spectral features can be distinguished between 8 and 12 μm for some materials using the LIP and FSP. These results

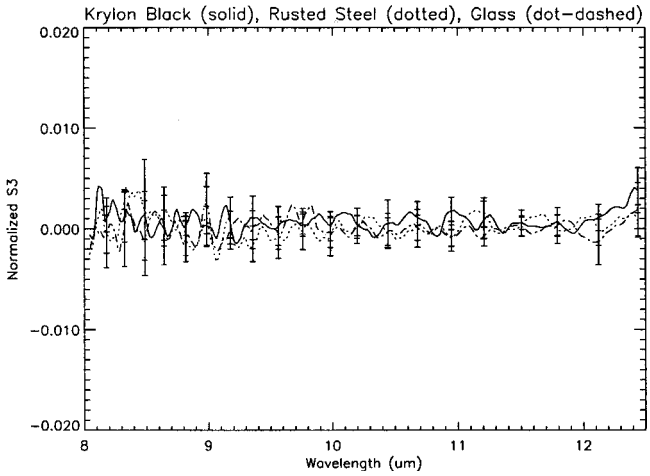

Fig. 14 Normalized $S3$ from three samples measured by the FSP at the Kirtland tower. Krylon black: solid line. Rusted steel: dotted line. Glass: dot-dashed line.

demonstrate that we are able to make polarization measurements that agree within a relative accuracy of 0.5% DOP between the two instruments, and that polarimetry has a great potential to enhance material identification and discrimination capabilities.

Acknowledgment

The authors would like to acknowledge the Air Force Office of Scientific Research for its support of this work.

References

1. F. Arago, *Ann. Chem. et Phys* **2**, 27 (1824).
2. R. A. Millikan, ''A study of the polarization of the light emitted by incandescent solid and liquid surfaces,'' *Phys. Rev.* **3**, 81–99, 177–192 (1895).
3. T. J. Rogne, F. G. Smith, and J. E. Roce, ''Passive target detection using polarized components of infrared signatures,'' *Proc. SPIE* **1371**, 242–251 (1990).
4. J. A. Shaw, ''Degree of linear polarization in spectral radiances from water-viewing infrared radiometers,'' *Appl. Opt.* **38**(15), 3157–3165 (1999).
5. R. A. Chipman, ''Polarimetry'' in *Handbook of Optics Vol. II*, Chap. 22, McGraw-Hill, New York (1995).
6. E. Collett, *Polarized Light: Fundamentals and Applications*, Marcel Dekker, New York (1993).
7. J. Boger, ''Calibration technique of a quarter-wave retarder,'' AFRL/DE Informal Technical Report, Applied Technology Associates (May 1997).
8. D. R. Anderson, D. J. Sweeney, and T. A. Williams, *Statistics for Business and Economics*, Chap. 8, West Publishing Company, Los Angeles (1990).
9. E. A. Sornsin and R. A. Chipman, ''Alignment and calibration of an infrared achromatic retarder using FTIR Mueller matrix spectropolarimetry,'' *Proc. SPIE* **3121**, 28–31 (1997).
10. M. H. Smith, J. D. Howe, J. B. Woodruff, and M. A. Miller, ''Multispectral infrared Stokes imaging polarimeter,'' *Proc. SPIE* **3754**, 138–143 (1999).

Stephanie H. Sposato, a captain in the US Air Force, is a research physicist for the Air Force Research Laboratory working in the Space Vehicles Spectral Polarimetry Program. She received a BS in physics from Rensselaer Polytechnic Institute in 1994, and a PhD in Physics from Washington University in Saint Louis in 1999. She previously worked in the field of experimental astrophysics, building high-altitude balloon-borne cosmic ray experiments. Her current work involves multispectral polarization imaging in the visible and LWIR wavebands, particularly polarization phenomenology data acquisition and analysis.

Matthew P. Fetrow is a senior engineer at Utah State University assigned to the Air Force Research Laboratory. He received his BS in physics from Utah State University in 1989 and an MBA from the University of Massachusetts in 1994. His technical work has primarily involved the development of infrared imaging systems and spectrometers. Most recently he has been involved in multispectral polarization imaging in the visible and LWIR bands. Polarization phenomenology has been a primary topic of his research.

Kenneth P. Bishop is an optical systems engineer at Applied Technology Associates. He received his BS in electrical engineering technology from DeVry Institute of Technology in 1988 and an MSEE from the University of New Mexico in 1992. His past technical work has involved research in optical propagation through turbulence and optical scattering. He is currently involved in multispectral polarization imaging in the visible and LWIR wavebands. The focus of his work is in instrument development, data acquisition, and data analysis for polarization phenomenology research.

Thomas R. Caudill is a research scientist and the leader of the Spectral Polarimetry Program of the Space Vehicles Directorate at the Air Force Research Laboratory. His research activities have concentrated on the phenomenology and modeling of atmospheric and cloud effects on remote sensing platforms in the visible and infrared portions of the spectrum. He received a BA in chemistry in 1984 from the University of Colorado, and a PhD in atmospheric science from the University of Arizona in 1995. His graduate work in atmospheric radiation included the development of a new polarized, spherical-geometry radiative transfer model.